This is the accepted version of the following article:
Wilding, B.V. and Beyer, K. (2018), Prediction of stiffness, force and drift capacity of modern in-plane loaded URM walls. Mauerwerk, 22: 77-90, which has been published in final form at https://doi.org/10.1002/dama.201800001

Bastian Valentin Wilding & Katrin Beyer:

Prediction of stiffness, force and drift capacity of modern in-plane loaded URM walls

Bastian Valentin Wilding[1]
bastian.wilding@epfl.ch

Katrin Beyer[1] – corresponding author
katrin.beyer@epfl.ch

[1]Earthquake Engineering and Structural Dynamics Laboratory (EESD), School of Architecture, Civil and Environmental Engineering (ENAC), École Polytechnique Fédérale de Lausanne (EPFL), EPFL ENAC IIC EESD, GC B2 504, Station 18, 1015 Lausanne, Switzerland

Abstract

Unreinforced masonry (URM) walls show a limited horizontal in-plane deformation capacity, which can lead to an unfavorable seismic response. To predict this response, the walls' effective stiffness, shear force and drift capacity are required. While mechanics-based models for the force capacity are well established, such approaches are largely lacking for the effective stiffness and the drift capacity. The mostly empirical code equations for the two latter parameters lead to often unsatisfactory and, in the case of drift capacities, sometimes unconservative predictions when compared to test results. This article summarises recently developed simple closed-form equations for the effective stiffness, the shear force and the drift capacity. Furthermore, it compares said formulations and currently used code equations to a database of shear compression tests. It shows that the novel models capture the effective stiffness and the drift capacity more accurately than current code equations. The shear force capacity is predicted with a similar reliability, yet using a very simple formulation.

Keywords: unreinforced masonry (URM) wall, force-displacement behaviour, shear force capacity, effective stiffness, drift capacity

1 Introduction

Nowadays, masonry construction is mainly used in residential buildings due to its good insulation capacities and a fair compressive strength. A downside of the material is its relatively high weight and limited deformation capacity in shear, which leads to a rather unfavorable response when subjected to seismic action [1], [2]. The in-plane response of URM walls is still not fully understood and despite a multitude of existing models (e.g. [3]–[6]), simple mechanical formulations that predict the effective stiffness and the (interstorey) drift capacity of shear and flexure controlled walls to be used in design are still lacking. In here, drift is the horizontal displacement divided by the storey height, which is supposed to be equal to the wall height for simplicity. This paper presents equations for the parameters needed to describe the in-plane force-displacement response of URM walls by means of bi-linear curves: the effective stiffness (k_{ef}), the shear force (V_P) and the drift capacity (δ_{ult}), see Figure 1. First, different approaches of determining the shear force capacity are revisited and new equations proposed. Subsequently, the initial stiffness, the ratio of shear to elastic modulus and the computation of the effective stiffness are treated. Formulations based on Wilding & Beyer [7], [8] are proposed and compared to recently used code approaches. Furthermore, a mechanics-based model for the ultimate drift capacity as developed in Wilding & Beyer [8], [9] is presented along with code approaches for this key parameter. All models are validated with results from a database [9] of 61 shear-compression tests.

2 Shear force capacity

Mechanical models for the shear force capacity are well established. Most of today's codes are based on one or several of the following four approaches for determining the peak shear capacity of in-plane loaded URM walls:

the Mohr-Coulomb (MC) criterion, the Turnšek-Čačovič (TC) criterion [10], the toe crushing/overturning criterion and finally a stress field criterion, which can be found in the Swiss code [11], [12].

2.1 Standard approaches

The MC criterion, which represents a bed-joint sliding failure, can be written in the following form:

$$V_{MC} = \lambda_2 \left(\underline{\mu} N + \underline{c}\, \lambda_1 L T \right) \tag{1}$$

Where T is the wall thickness, L the wall length, N the normal force, $\underline{\mu}$ the global friction coefficient, $\underline{c}$ the global cohesion and the λ_i are factors taking into account possible modifications of this formula in the literature [13]–[16]. The TC equation can be written as given in Eq. (2), again making use of parameters λ_i to account for various modifications in different literature sources [10], [15], [16]. This criterion describes the condition for a diagonal tensile cracking failure of the masonry due to shear.

$$V_{TC} = \lambda_3 f_{dt} L T \sqrt{1 + \lambda_4 \frac{\sigma_0}{f_{dt}}} \tag{2}$$

Where f_{dt} is the diagonal tensile strength of masonry and σ_0 the axial stress. Toe crushing and/or overturning criteria are also employed in many codes [13]–[15] to account for flexural failure of the wall. It can be generally written as follows, again, using factors λ_i representing different versions of the formulation:

$$V_{TO} = \frac{NL}{2(H_0 - \lambda_5)} \left(1 - \lambda_6 \frac{\sigma_0}{f_u} \right) \lambda_7 \tag{3}$$

Where N is the normal force on the wall, H_0 the shear span measured from the wall base and f_u the masonry compressive strength. The factors λ_i are summarized for various literature sources in Table 1.

2.2 Swiss code

The Swiss masonry code SIA 266 [12] evaluates the shear force capacity of in-plane loaded URM walls using a stress field approach developed by Ganz [17] superposing an inclined and a vertical stress field. A sketch of the system is shown in Figure 2. The seismic guideline SIA D 0237 [11] provides capacity and equilibrium equations describing the superposed vertical and inclined stress fields. The equations can be combined and re-arranged to Eq. (4), which simply has to be evaluated for multiple angles α. The value of α that leads to the maximum shear force is closest to the actual shear force capacity.

$$V(\alpha) = \frac{-f_a^2 f_m f_v H_0 + f_a f_v N + (f_m + f_v) \sqrt{\frac{f_a^2 f_m f_v \{ f_a^2 f_m f_v H_0^2 - 2 f_a f_v H_0 N + [(f_m + f_v) L - N]\, N \}}{(f_m + f_v)^2}}}{f_m + f_v} \tag{4}$$

With: $f_a = \tan(\alpha)$, $f_m = (f_u - f_y)\, T$, $f_v = f_y\, T \cos^2(\alpha)$ where f_y is the masonry compressive strength perpendicular to the head-joints and α the angle of the inclined stress field, which is iterated from 0 to atan(μ), where μ is the local friction coefficient, in order to find the maximum shear force capacity.

2.3 Shear-normal stress failure domains

Figure 3 presents shear-normal stress failure domains for walls with parameters following the specimens tested by Petry & Beyer [18], see also Table 2. For the MC and the TC criterion, the λ-values are set equal to one, while for the toe crushing equation the parameters λ_i are set to $\lambda_5 = h_B$ (h_B is the brick height) and $\lambda_6 = \lambda_7 = 1$ representing the point at which a full plastic stress block at the second bed-joint has emerged. Furthermore a 'practical limit' for a axial load ratio (σ_0 / f_u) range in-between 5 and 30 % is indicated. For Figure 3a, showing a wall with a shear span-to-wall height ratio of 0.5, the predicted failure mode gradually changes with increasing normal force from an overturning failure for very low axial loading to bed-joint sliding to diagonal cracking of the masonry to a compressive failure of the masonry for a high axial load ratio. In Figure 3b, illustrating a shear span of 1.0 H, the only governing criterion is overturning/toe crushing for the chosen set of parameters.

As for the stress field criterion according to the Swiss code [12] [Eq. (4)], also illustrated in Figure 3, it yields nearly equivalent results within the indicated practical limits for both considered configurations. However, for higher axial loads and a shear span of 0.5 times the wall height (Figure 3a), the stress field criterion may lead to lower estimates than the other formulations for the considered parameter set. In the case of a shear span-to-wall height ratio of one as shown in Figure 3b, the overturning/toe crushing equation and the stress field criterion match.

2.4 Proposed equations

2.4.1 Shear failure

It is proposed to evaluate the capacity of a wall failing in shear simply using $V = N/2$. This relation corresponds to a MC criterion with zero cohesion and a friction coefficient of 0.5. This formulation is already used in ASCE 41 [14] as one of the two equations governing shear failure. Unlike other MC criteria, it does not require any more specific knowledge of the friction coefficient and the cohesion, which are sometimes not available and not even determined in testing campaigns. Moreover, there is a fairly large difference between the local friction coefficient measured in small-scale friction tests and the global one to be used in MC criteria evaluating a section of the wall. The global friction coefficient can be derived from the local one using the model by Mann and Müller [16] but it requires assumptions of the torque stress distribution at the brick level for which different ones are possible [19]–[21]. The TC criterion evaluating diagonal tensile failure in the wall requires the diagonal tensile strength of masonry, which is not always available either. However, all said criteria have in common that as the normal force on the wall increases, the shear force capacity increases too. This trend can also be clearly observed in experiments [18], [22]. In other words, the shear capacity equations all work provided the right strength values are used.

Figure 4a shows a comparison of the above-mentioned approaches to a database of shear-compression tests [9]. The database contains the results of 61 quasi-static cyclic shear-compression tests. The specimens comprise walls made of clay, calcium-silicate and aerated concrete units with normal strength mortar and thin as well as normal thickness bed-joints and were tested by [18], [22]–[27]. The EC8-approach [13], the equations provided in ASCE 41 [14] and the suggested formulation show roughly the same performance in predicting the shear force capacity of walls the respective approach grades shear controlled. In Figure 4b, the shear-normal stress curves from Figure 3a are shown, this time including the proposed criterion. For the considered set of parameters, the MC formulation and the suggested criterion lie nearly on top of each other. Yet the criterion may slightly underestimate the force capacity for low axial load ratios and overestimate it for high normal forces.

2.4.2 Flexural failure

To evaluate the force capacity of walls failing in flexure, two overturning/toe crushing equations are proposed that have already been introduced in [8]. The first yields the shear force at which a full plastic stress block has formed in the second bed-joint.

$$V_{cru1} = \frac{NL}{2(H_0 - h_B)}\left(1 - \frac{\sigma_0}{f_u}\right) \tag{5}$$

The second relation gives the shear force at which the brick compressive strength ($f_{B,c}$) is reached in the outermost fibre at the wall base.

$$V_{cru2} = \frac{NL}{2H_0}\left(1 - \frac{4}{3}\frac{\sigma_0}{f_{B,c}}\right) \tag{6}$$

The overall shear force capacity of an in-plane loaded URM wall is proposed to be determined taking the minimum of the above-mentioned relations capturing shear and flexural failure.

$$V_P = \min\left[\frac{N}{2}, V_{cru1}, V_{cru2}\right] \tag{7}$$

2.5 Comparison

The proposed approach and code provisions for predicting the shear force capacity are compared to the shear-compression test database [9] in Figure 5. For calculations according to SIA D 0237 [11], the following assumptions are made: the compressive strength perpendicular to the head joints $f_y = 0.3\, f_u$ [17], [28]. Furthermore, the local coefficient of friction and the cohesion from small-scale tests are transformed to global ones for calculations according to EC8 [13] using the relations suggested in Mann and Müller [16]. For the computations according to ASCE 41 [14] and SIA [11], [12], however, local values for the friction coefficient and the cohesion are used. This is done as ASCE 41 requires explicitly the *average of the bed-joint shear strength test values* to be used and since the stress field criterion in the Swiss code does not evaluate a whole section but rather a localized zone where the inclined and the vertical stress fields intersect. All code approaches show a fairly good agreement with the test results. The proposed approach leads to a similarly good fit while not needing any knowledge of friction coefficient, cohesion or diagonal tensile strength of masonry.

3 Effective stiffness

When evaluating shear-compression tests, the effective stiffness is often defined as the stiffness of the system at 70% the shear force capacity, while for prediction purposes, the effective stiffness is typically estimated as a fixed percentage of the initial wall stiffness [11], [29]. The initial stiffness is usually determined based on Timoshenko beam theory, which requires as input the elastic and the shear modulus of masonry. In testing campaigns, the elastic modulus can be obtained from compression tests, while codes provide equations for the elastic modulus using a fixed multiple of the masonry compressive strength. The determination of the shear modulus by means of tests, however, is not unified. Codes propose the shear modulus to be determined as a fixed percentage of the elastic modulus [30], [31].

3.1 Ratio of shear and elastic modulus

Many codes ([12], [15], [30], [31]) propose a ratio of elastic to shear modulus of 0.4. According to TMS 402 [31] this is not based on any scientific evidence but rather on historic convenience. The ratio has already been put into question by Tomaževič [32], who also suggests a simple approach for estimating the G/E ratio from experimental results which is outlined in the following. If the elastic modulus has been determined from masonry compression tests, the shear modulus can be retrieved from shear-compression tests with said elastic modulus and the measured initial stiffness using Timoshenko beam theory.

Applying this approach to five shear-compression tests, a G/E ratio of 0.1 is proposed by Tomaževič [32]. In this article, the suggested approach of estimating the shear modulus is used for walls tested by Petry & Beyer [18] (Table 2). The initial stiffness is taken as the measured stiffness of the system between 5 and 20 % of the shear force capacity. Figure 6 presents the results by means of a G/E vs axial load ratio plot. It shows that five of the six considered wall tests lead to a G/E ratio of around 0.25, which seems to confirm the assumption made in the following to use $G = 0.25\ E$ as already done in [5].

3.2 Initial elastic modulus of masonry

According to Eurocode 6 (EC6) Part 1 [30], the elastic modulus of masonry can be obtained with $E = 1000\ f_{u,k}$. Where $f_{u,k}$ is the characteristic masonry compressive strength, which can be back-calculated from the mean strength f_u using the proposal by EN 1052-1 [33]: the mean strength is 20% larger than the characteristic one. This results in $E = 833\ f_u$. Furthermore EC6 suggests the shear modulus be taken as: $G = 0.40\ E$. ASCE 41 [14] refers to TMS 402 [31], which specifies $E = 700\ f_u$ for clay masonry and $E = 900\ f_u$ for concrete masonry. Furthermore, TMS 402 states, in line with EC6 [30], that the shear modulus shall be taken as 40 % of the elastic one but indicates that this is a historically used relationship with no experimental evidence supporting it.

In this paper, the following empirical relation for the initial elastic modulus of masonry dependent on the axial load ratio and the masonry compressive strength for the initial elastic modulus is proposed. It is based on an analysis of a database of shear-compression tests [7], which showed a dependency of the initial stiffness of in-plane loaded URM walls on the applied axial load ratio.

$$E_{init} = \alpha\ f_u \left(1 + \beta \frac{\sigma_0}{f_u}\right) \tag{8}$$

Where $\alpha = 470$ for clay brick and $\alpha = 720$ for calcium-silicate brick masonry walls while $\beta = 4$ for both types with a G/E ratio of 0.25. The performance of Eq. (8) in predicting the initial E-modulus of wall tests from the database [9], is compared to code formulations estimating the initial elastic modulus simply as a multiple of the masonry compressive strength. For the proposed approach, the initial elastic moduli of the wall tests are back-calculated from the measured initial stiffness using a G/E ratio of 0.25 while for the EC6-approach [30] and the provision according to TMS 402 [31] they are obtained using a G/E ratio of 0.4 as suggested by the respective codes in order to remain consistent throughout the whole prediction process. Figure 6b shows that both code formulations over-estimate the initial elastic modulus while the proposed approach shows a good median fit and a lower dispersion.

3.3 Effective to initial stiffness ratio

In EC8 Part 1 [29] it is suggested that, *in absence of an accurate evaluation of the stiffness properties*, 50 % of the gross sectional elastic stiffness be taken as an effective stiffness estimate. ASCE 41 [14] simply states that flexural and shear deformations shall be considered with an elastic modulus as specified by TMS 402 [31]. No mention is made about effective or cracked stiffnesses of the wall. Therefore, the provided un-cracked (initial) stiffness is used for comparison below. According to the Swiss code [11], [12], [34], the characteristic elastic modulus can be obtained with the relation $E_k = 1000\ f_{u,k}$, while G/E is 0.4. Both elastic and shear modulus are proposed to be reduced by 70 % to obtain the effective wall stiffness.

According to the analytical model developed by Wilding & Beyer [7], [8] which accounts for the reduction in stiffness due to uplift in bed-joints and diagonal cracking of the wall, the effective stiffness is around 75 % of the initial wall stiffness. This is in agreement with an analysis of shear-compression tests [7]. Therefore it is recommended to use 75 % of the initial stiffness as an effective stiffness estimate. Figure 7 illustrates the performance of the considered code approaches [11], [14], [30] and the introduced formulation in predicting the effective stiffness of the wall tests from the database [9]. Both the presented approach and the EC8-formulation show a good median fit, the provision according to EC8, however, with a larger deviation. The Swiss code significantly underestimate the median effective stiffness, while the American code overestimates it fairly strongly.

Concerning the EC8-approach [29], it may be worthy adding that despite the good median fit of the provision concerning the effective stiffness, the approach is based on three assumptions that appear not to be entirely correct for the investigated masonry typologies. First, the proposed G/E ratio of 0.4 appears to be too high for masonry walls as already stated by [32] and indicated further in Figure 6a. Second, the formulation for the initial elastic modulus based on the multiple of the masonry compressive strength ($E_{init} = 833\, f_u$), along with the G/E ratio of 0.4, leads to an initial stiffness that is too high, Figure 6b. Finally, the provision of taking half of the initial stiffness to estimate the effective (cracked) one appears to be too low as the initial-to-effective stiffness ratio seems rather to be found around 0.75. However, the assumptions' deficiencies seem to cancel each other out when estimating the effective stiffness—an initial stiffness that is too high is reduced by a factor that is too low—leading to a rather good median fit in predicting the above-mentioned test results.

4 Ultimate drift

The ultimate drift of a shear-compression wall test is often defined as the point in the post-peak domain at which the shear force has decreased by 20% [35]. There are roughly two prediction approaches to be found in codes. The first one provides fixed values for the drift, possibly multiplied by a geometrical ratio, only changing with the predicted wall failure mode. The second approach neglects the failure mode and relates the drift capacity to the axial load ratio. Three code provisions, two corresponding to the former and one to the latter approach, are briefly described below.

4.1 Code equations

EC8 Part 3 [13] gives an estimate of the drift at the *Limit State of Near Collapse*. For walls failing in shear, the drift capacity is set to a constant value ($\delta_{ult} = 4/3\ 0.4$ [%]) while the one for flexure controlled walls is given as a base value times the shear span ratio: $\delta_{ult} = 4/3\ 0.8\ H_0 / L$ [%]. According to the Swiss guideline SIA D 0237 [11], the *deformation capacity* of the wall is to be determined taking into account the boundary conditions a wall is subjected to without considering the predicted failure mode. The relation, which is based on the work of Lang [28], can be given as follows.

$$\delta_{ult} = 0.8\ [\%] \left(1 - \frac{\sigma_0}{f_u}\right) \frac{H_0}{H} \tag{9}$$

The American standard ASCE 41 [14] provides the drift (among others) at the *Performance Limit of Life Safety*, which is supposed to be approximately equal to the ultimate drift capacity. For bed-joint sliding failure a constant drift limit of 0.75 % is provided. Yet for rocking failure, the provision states: $\delta_{ult} = 100\ u_{tc,r} / H$ with $u_{tc,r}$ being the drift *associated with the onset of toe crushing*, smaller or equal to 2.25 %. Furthermore it reads in the commentary section: *The deformation associated with the onset of toe crushing shall* [...] *be* […] *established and checked* […] *using a moment-curvature or similar analytical approach.* This appears to indicate that the engineer is free to choose any analytical approach in order to *establish* the required deformation limit $u_{tc,r}$. Another hint related to rocking walls is provided in the commentary section of ASCE 41 saying: *The test results indicate* […] *drifts of at least* 1.5 % *are sustainable for certain configurations* […]. In order to consistently compare code provisions without having to resort to models not included in said codes, the drift limit of 1.5 %, as mentioned in the commentary, is used for walls showing a rocking failure.

4.2 Proposed model

It is suggested to use the mechanics-based relation introduced in Wilding & Beyer [8], [9] for estimating the ultimate drift of an in-plane loaded URM wall.

$$\delta_{ult} = \left(\max\left\{\min\left[\frac{f_{B,c}}{E}; 0.007\right]; 0.004\right\} - \frac{\sigma_0 L}{E l_B}\right) \frac{h_{cr}}{l_B} \left(1 - \frac{h_{cr}}{3H}\right) \tag{10}$$

Where $h_{cr} = \max\left[h_B\ (0.5 + H_0 / H)\ ; T\right]$ and l_B is the brick length. Equation (10) evaluates the integral of a triangular curvature distribution at the wall base representing a crushed zone at the wall toe at ultimate failure. A similar

concept has already been put forward by Priestley et al. [36] for flexure controlled walls. Yet solely a constant base curvature and height of the curvature distribution were considered in [36] leading to a constant prediction of the drift capacity notwithstanding changing support or loading conditions. Equation (10), on the contrary, relates a change in boundary conditions to varying base curvatures and curvature distribution heights. Furthermore the proposed formulation may be used for shear and flexure controlled walls.

4.3 Comparison

Figure 8 compares the performance of the novel approach in predicting the results of the database [9] to the fit of the code provisions. All approaches show a large scatter. The EC8 [13] and ASCE 41 [14] predictions are mainly too high, while the SIA-formulation [11] and the equation proposed in here show a rather good median fit, both however with a large dispersion.

As visible in Figure 8a, tests with drift capacities of more than 1 % are largely underestimated by the considered approaches, which, at least, results in predictions on the safe side for those cases. Walls with a drift capacity larger than 1 % are typically characterized by a low axial load ratio. Yet these types of walls do usually not govern the force-displacement response of a building as they only carry a small share of the total normal force. When neglecting tests with drift capacities larger than 1 %, the fit of the proposed formulation can be significantly improved as is shown in Figure 9, while the EC8, the ASCE 41 and now also the SIA formulations all lead to a significant overestimation of the drift capacities. Figure 9a illustrates, furthermore, that the proposed approach and slightly less so the SIA formulation appear to capture most trends in drift capacity development as the data points line up in vicinity of the diagonal perfect-fit-line. The EC8 and ASCE 41 provisions seem not to capture important trends.

5 Conclusion

This article addresses the computation of the effective stiffness, the force and the drift capacity of modern in-plane loaded URM walls focusing on approaches that are suitable for engineering practice. It proposes standalone formulations and compares them to code equations. Concerning the shear force capacity, it is suggested to use the minimum of two toe crushing criteria, evaluating crushing in the first and second brick row respectively, and a simplified Mohr-Coulomb equation. With regard to the stiffness of in-plane loaded URM walls, first the G/E ratio is discussed and it is suggested to use a value of 0.25 rather than the currently used 0.4. Second a formulation for the initial elastic modulus based on the masonry compressive strength and the axial load ratio is introduced and, third, an effective-to-initial stiffness ratio of 0.75 proposed. A mechanics-based stand-alone equation for the ultimate drift capacity, evaluating a crushed zone with large curvatures at the wall toe, is suggested. Finally, all proposed formulations along with code provisions from EC8 [13], ASCE 41 [14] and the Swiss code [11] are compared to a database of 61 full-scale shear-compression tests on modern URM walls. It shows that the effective stiffness and the drift capacity are predicted more accurately by the suggested novel formulae than by any of the considered codes.

However, there are some limitations to the introduced formulations. They are only validated for a restricted number of masonry typologies with a fairly small number of tests. Further work validating the proposed equations with more typologies may be required once such tests become available. Moreover, a centric application of the normal force on the wall is assumed in all cases. Yet an eccentric vertical force might influence both shear force and drift capacities.

6 Acknowledgement

This study has been supported by the grant no. 159882 of the Swiss National Science Foundation: “A drift capacity model for unreinforced masonry walls failing in shear”.

7 References

[1] D. P. Abrams, “Performance-based engineering concepts for unreinforced masonry building structures,” *Prog. Struct. Eng. Mater.*, vol. 3, no. 1, pp. 48–56, Jan. 2001.

[2] G. Magenes, “Masonry Building Design in Seismic Areas: recent experiences and prospects from a European standpoint,” in *Proceedings of the 1st European Conference on Earthquake Engineering and Seismology*, 2006.

[3] A. Benedetti and E. Steli, “Analytical models for shear–displacement curves of unreinforced and FRP reinforced masonry panels,” *Constr. Build. Mater.*, vol. 22, no. 3, pp. 175–185, Mar. 2008.

[4] A. Penna, S. Lagomarsino, and A. Galasco, “A nonlinear macroelement model for the seismic analysis of masonry buildings,” *Earthq. Eng. Struct. Dyn.*, vol. 43, no. 2, pp. 159–179, Feb. 2014.

[5] S. Petry and K. Beyer, “Force-displacement response of in-plane-loaded URM walls with a dominating flexural mode,” *Earthq. Eng. Struct. Dyn.*, vol. 44, no. 14, pp. 2551–2573, Nov. 2015.

[6] I. Caliò, M. Marletta, and B. Pantò, “A new discrete element model for the evaluation of the seismic behaviour of unreinforced masonry buildings,” *Eng. Struct.*, vol. 40, no. October 2015, pp. 327–338, Jul. 2012.

[7] B. V. Wilding and K. Beyer, “The effective stiffness of modern unreinforced masonry walls.,” *Submitt. to Earthq. Eng. Struct. Dyn.*, 2017.

[8] B. V. Wilding and K. Beyer, “Force–displacement response of in-plane loaded unreinforced brick masonry walls: the Critical Diagonal Crack model,” *Bull. Earthq. Eng.*, vol. 15, no. 5, pp. 2201–2244, May 2017.

[9] B. V. Wilding and K. Beyer, “The drift capacity of modern unreinforced masonry walls.,” *Submitt. to Earthq. Eng. Struct. Dyn.*, 2017.

[10] V. Turnšek and F. Čačovič, “Some experimental results on the Strength of Brick Masonry Walls,” in *Proceedings of the 2nd International Brick and Block Masonry Conference*, 1970.

[11] SIA, “SIA D 0237: Evaluation de la sécurité parasismique des bâtiments en maçonnerie (Seismic assessment of masonry buildings),” Swiss Society of Engineers and Architects, Zürich, Switzerland, 2011.

[12] SIA, “SIA 266: Masonry,” Swiss Society of Engineers and Architects, Zürich, Switzerland, 2015.

[13] CEN, “EN 1998-3:2005 Eurocode 8: Design of structures for earthquake resistance - Part 3: Assessment and retrofitting of buildings,” European Committee for Standardization, Brussels, Belgium, 2005.

[14] ASCE, *ASCE 41-13: Seismic Evaluation and Retrofit of Existing Buildings*. Reston, VA: American Society of Civil Engineers, 2014.

[15] NZSEE, “The Seismic Assessment of Existing Buildings: Technical Guidelines for Engineering Assessments,” New Zealand Society for Earthquake Engineering, Wellington, New Zealand, 2016.

[16] W. Mann and H. Müller, “Failure of shear-stressed masonry. An enlarged theory, tests and application to shear walls,” *Proc. Br. Ceram. Soc.*, vol. 30, pp. 223–235, 1982.

[17] H. Ganz, “Mauerwerksscheiben unter Normalkraft und Schub,” PhD-Thesis, ETH Zürich, 1985.

[18] S. Petry and K. Beyer, “Cyclic Test Data of Six Unreinforced Masonry Walls with Different Boundary Conditions,” *Earthq. Spectra*, vol. 31, no. 4, pp. 2459–2484, Nov. 2015.

[19] R. H. Atkinson, B. P. Amadei, S. Saeb, and S. Sture, “Response of Masonry Bed Joints in Direct Shear,” *J. Struct. Eng.*, vol. 115, no. 9, pp. 2276–2296, 1990.

[20] P. B. Lourenço, “Computational strategies for masonry structures,” PhD-Thesis, TU Delft, 1996.

[21] B. Elsche, “Zur rechnerischen Modellierung der Beanspruchungen und der Tragfähigkeit von aussteifenden Mauerwerkswänden,” PhD-Thesis, TU Dortmund, 2008.

[22] A. H. Salmanpour, N. Mojsilović, and J. Schwartz, “Displacement capacity of contemporary unreinforced masonry walls: An experimental study,” *Eng. Struct.*, vol. 89, pp. 1–16, Apr. 2015.

[23] V. Bosiljkov, M. Tomaževič, and M. Lutman, “Optimization of shape of masonry units and technology of construction for earthquake resistant masonry buildings - Part Three,” Research Report, ZAG Lubljana, Slowenia, 2006.

[24] V. Bosiljkov, M. Tomaževič, and M. Lutman, “Optimization of shape of masonry units and technology of construction for earthquake resistant masonry buildings - Part One and Two,” Research Report, ZAG Lubljana, Slowenia, 2004.

[25] H. Ganz and B. Thürlimann, “Versuche an Mauerwerksscheiben unter Normalkraft und Querkraft,” Test Report Nr. 7502-4, ETH Zürich, 1984.

[26] A. Ötes and S. Löring, “Zum Tragverhalten von Mauerwerksbauten unter Erdbebenbelastung,” *Bautechnik*, vol. 83, no. 2, pp. 125–138, Feb. 2006.

[27] G. Magenes, P. Morandi, and A. Penna, “D 7.1c Test results on the behaviour of masonry under static cyclic in plane lateral loads,” Test Report, ESECMaSE Poject, University of Pavia, EURCENTRE, Italy, 2008.

[28] K. Lang, “Seismic vulnerability of existing buildings,” PhD-Thesis, ETH Zürich, 2002.

[29] CEN, “EN 1998-1:2004 Eurocode 8: Design of structures for earthquake resistance - Part 1: General rules, seismic actions and rules for buildings,” European Committee for Standardization, Brussels, Belgium,

2004.

[30] CEN, “EN 1996-1-1:2005 Eurocode 6: Design of masonry structures - Part 1-1: General rules for reinforced and unreinforced masonry structures,” European Committee for Standardization, Brussels, Belgium, 2005.

[31] TMS, “TMS 402: Building Code Requirements for Masonry Structures,” The Masonry Society, Boulder, Colorado, 2008.

[32] M. Tomaževič, “Shear resistance of masonry walls and Eurocode 6: shear versus tensile strength of masonry,” *Mater. Struct.*, vol. 42, no. 7, pp. 889–907, 2009.

[33] CEN, “EN 1052-1:1998-12 Methods of test for masonry - Part 1: Determination of compressive strength,” European Committee for Standardization, Brussels, Belgium, 2002.

[34] SIA, “SIA 269/8: Existing structures - Earthquakes,” Swiss Society of Engineers and Architects, Zürich, Switzerland, 2014.

[35] S. Frumento, G. Magenes, P. Morandi, and G. M. Calvi, “Interpretation of experimental shear tests on clay brick masonry walls and evaluation of q-factors for seismic design,” IUSS Press, Research Report EUCENTRE 2009/02, Pavia, 2009.

[36] M. J. N. Priestley, G. M. Calvi, and M. J. Kowalsky, *Displacement-based seismic design of structures*. Pavia, Italy: IUSS Press, 2007.

[37] G. Magenes and G. M. Calvi, “In-Plane Seismic Response of Brick Masonry Walls,” *Earthq. Eng. Struct. Dyn.*, vol. 26, pp. 1091–1112, 1997.

Figures

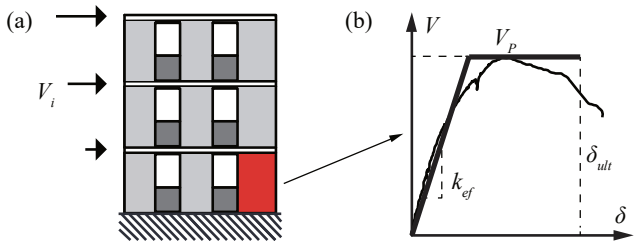

Figure 1: (a) Simplified 2D system of building under lateral loading, (b) envelop shear force-drift response of wall test [18] and possible bi-linear approximation

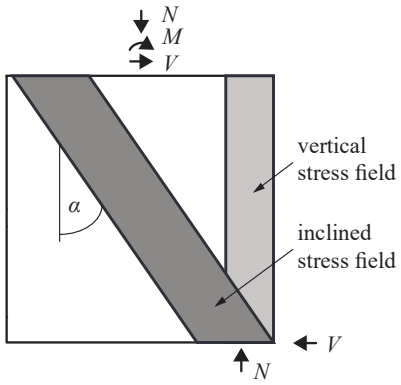

Figure 2: System with two superposed stress fields [11], [12]

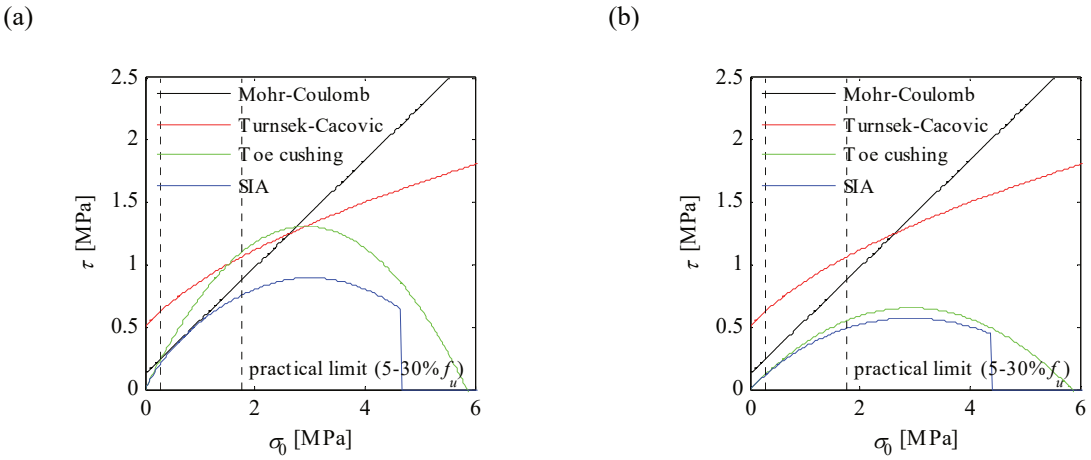

Figure 3: Shear-normal stress curves for wall with parameters as in [18] and a shear span of (a) 0.5 H and (b) 1.0 H [$\tau = V/(LT)$]

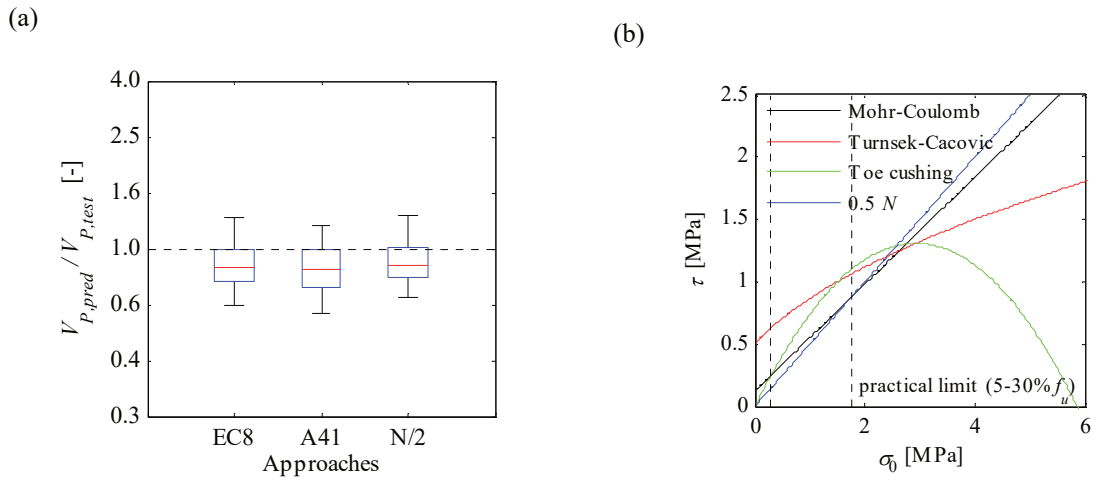

Figure 4: (a) Boxplot showing performance of approaches in predicting the shear force capacity of walls failing in shear (according to the respective approach). (b) Shear-normal stress curves for wall with parameters as in [18] and a shear span of 0.5 including proposed shear criterion [$\tau = V/(LT)$]

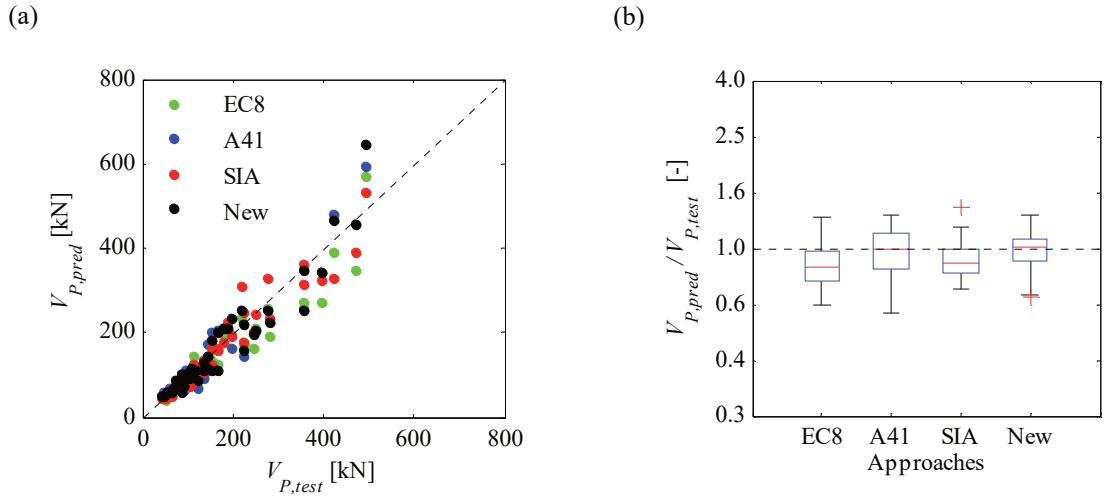

Figure 5: Comparison code approaches to predict shear force capacity of wall tests, (a) predicted vs measured peak shear capacity, (b) boxplot

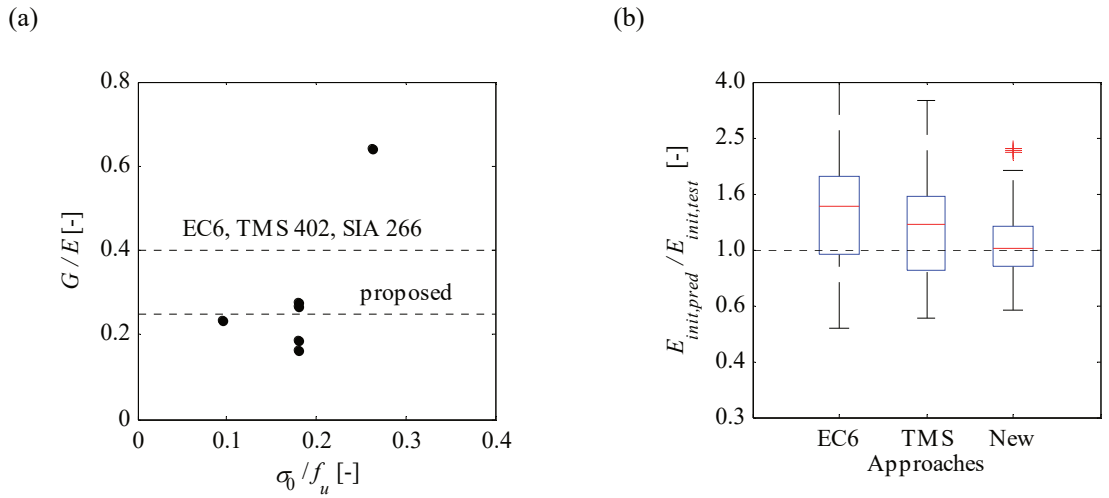

Figure 6: (a) G to E ratios back-calculated from test results in Petry & Beyer [18] vs axial load ratio. (b) Boxplots of predicted initial elastic modulus to experimentally determined elastic modulus for various approaches.

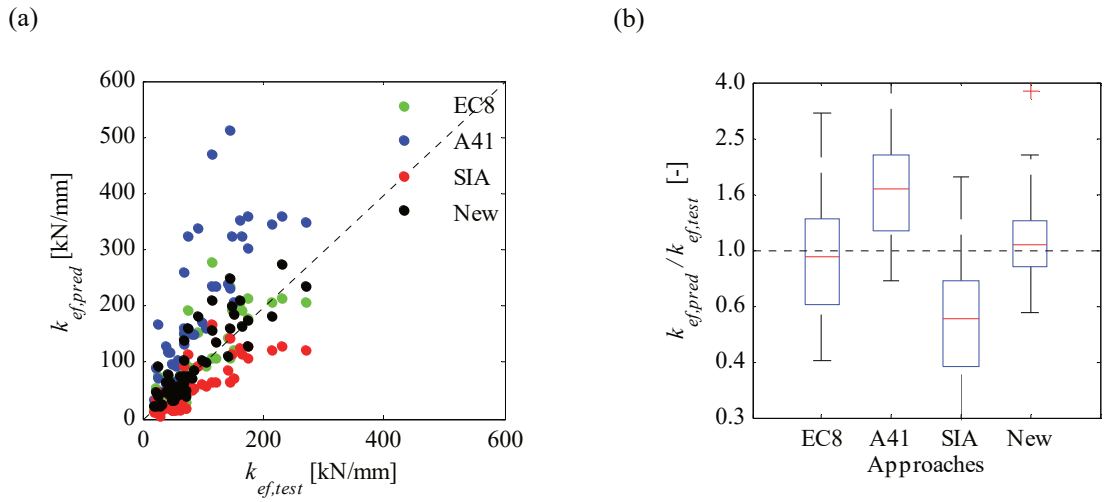

Figure 7: Comparison code approaches to predict the effective stiffness of wall tests, (a) predicted vs measured effective stiffness, (b) boxplot

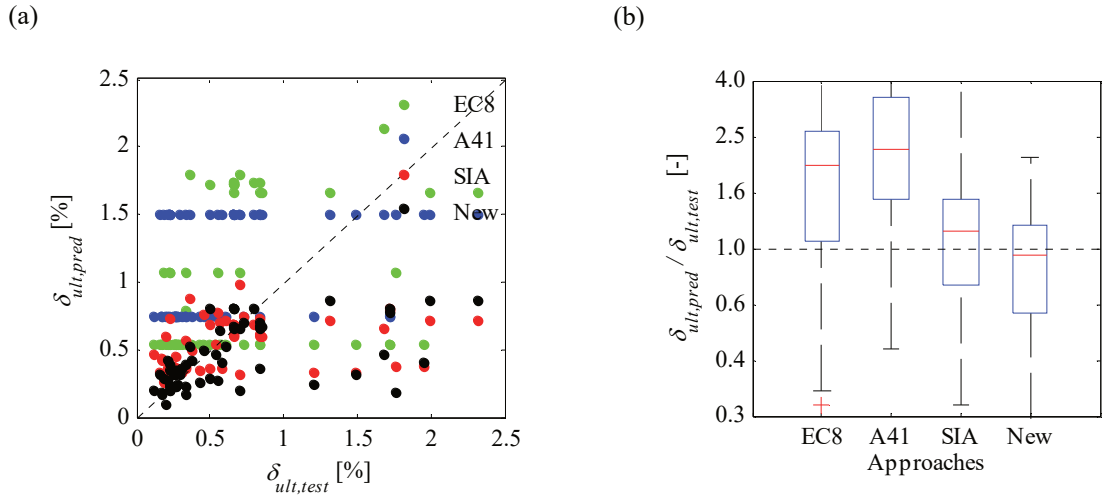

Figure 8: Comparison code approaches to predict ultimate drift capacity of wall tests (all wall tests considered), (a) predicted vs measured drift capacity, (b) boxplot

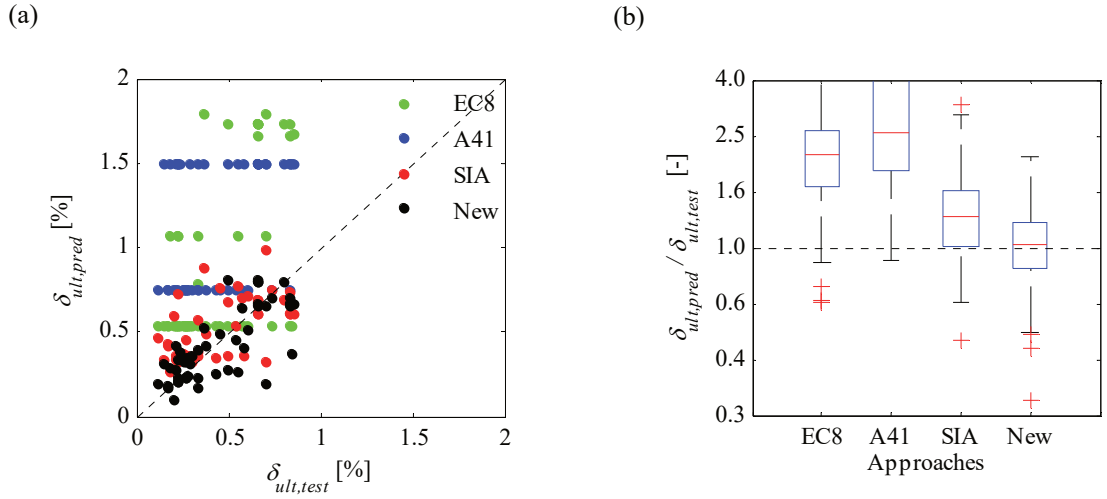

Figure 9: Comparison code approaches to predict ultimate drift capacity of wall tests (only tests with drift capacities smaller than 1 % are considered), (a) predicted vs measured peak shear capacity, (b) boxplot

Tables

Table 1: Values for λ_i according to different literature sources ($f_{B,t}$ is the tensile and $f_{B,c}$ the compressive brick strength)

	λ_1	λ_2	λ_3	λ_4	λ_5	λ_6	λ_7
EC8 [13]	L_c / L	1	-	-	0	1.15	1
ASCE 41 [14]	1	0.75/1.5	-	-	0	0	0.9
Turnsek & Cacovic [10]	-	-	1	1/1.5	-	-	-
Mann & Müller [16]	1	1)	$f_{B,t}$ /(2.3f_{dt})	f_{dt} / $f_{B,t}$	-	-	-
Magenes & Calvi [37]	L_c / L	1	2)	1	0	1/0.85	1
Petry & Beyer [5]	-	-	-	-	0	4/3 f_u / $f_{B,c}$	1

1) 1 for $H/L < 1$, 1/1.5 for $H/L > 1$
2) 1 for $H/L < 1$, 1/1.5 for $H/L > 1.5$

Table 2: Parameters following [18] as used to compare shear capacity equations in Figure 3 and Figure 4b (h_B is the height and l_B is the length of a brick)

H [mm]	L [mm]	T [mm]	l_B [mm]	h_B [mm]	μ [-]	c [MPa]	f_u [MPa]	$f_{B,c}$ [MPa]
2250	2010	200	300	190	0.94	0.27	5.86	35